Controls on circum-Antarctic grounding-line sinuosity

L.M. Simkins[1*], L. A. Stearns[2], K. L. Riverman[3,4]

[1]Department of Environmental Sciences, University of Virginia, Charlottesville, Virginia, USA

[2]Department of Geology, University of Kansas, Lawrence, Kansas, USA

[3]College of Earth, Ocean, and Atmospheric Sciences, Oregon State University, Corvallis, OR, USA

[4]Department of Environmental Studies, University of Portland, Portland, OR, USA

Corresponding author: Lauren Simkins (lsimkins@virginia.edu)

Key points:

- Sinuous grounding lines preferentially occur on low-sloping and low-roughness beds and where height-above-buoyancy gradients are shallow.
- Unpinned grounding lines experiencing ocean-forced retreat increase in sinuosity and retreat off pinning points leads to sinuosity loss.
- Grounding-line sinuosity reflects differential inland retreat, primarily of glacial systems near floatation and susceptible to retreat.

Keywords:

Ice sheet, grounding-line retreat, topography, bed slope, height above buoyancy, ice flux

Abstract

Mapping modern and paleo-grounding lines around the Antarctic Ice Sheet elucidates processes occurring at the grounded ice-ocean interface. Positional differences across individual grounding lines manifest as longitudinal (plan-view) grounding line sinuosity. We explore the causes and significance of such sinuosity by coupling observations of contemporary Antarctic grounding lines and paleo-grounding lines expressed as ice-marginal landforms, specifically focusing on the role that bed topography may play in influencing grounding-line sinuosity. For equal-length grounding-line segments, modern and paleo-grounding lines have remarkably similar sinuosity distributions, with the vast majority of grounding lines being near linear. Surprisingly, grounding line sinuosity is highest on low sloping beds and lower on rougher beds, even for grounding lines that are clearly pinned on topographic highs. For contemporary grounding

lines, sinuosity is higher and more variable for grounding lines near floatation with shallow height-above-buoyancy gradients. We argue that grounding line sinuosity is a product of the combined influence of height-above-buoyancy gradient, bed slope, and bed roughness and, perhaps counterintuitively, that this relationship does not appear to be sensitive to the presence of pinning points, ice-flow speed, or the presence/absence of an ice shelf.

Plain-language summary

The vast majority of ice-mass loss of the Antarctic Ice Sheet occurs where grounded ice goes afloat or produces icebergs in the ocean (i.e., the grounding line). Changes in the position of the hundreds of glacier and ice stream grounding lines are critical to understand as global sea-level rise in the future is coupled to the magnitude of ice thinning and inland retreat of grounding lines. This study characterizes the plan-view shape (i.e., sinuosity) of contemporary and paleo-grounding lines of the Antarctic Ice Sheet to determine the conditions that lead to more or less sinuous grounding lines and how the shape of grounding lines evolves through time. We find systematic relationships between configuration of glacial ice, the underlying terrain, and grounding-line sinuosity, where more sinuous grounding lines occur on relatively featureless (smooth, flat) beds and grounded ice is close to floatation limits. Increased grounding-line sinuosity fundamentally increases grounding line exposure to the ocean and potentially amplifies tidal processes, both of which may lead to retreat.

1 Introduction

Mass loss of the Antarctic Ice Sheet is largely driven by changes at the grounding line, the most downstream location where glacial ice is in contact with the underlying terrain (i.e., bed), before going afloat or calving (Thomas et al., 1979). Ocean-forced melt and ice-flow dynamic change can initiate grounding line retreat, which in turn leads to changes in ice-shelf cavity geometry, water column mixing, and upstream buttressing and ice flux at the grounding line (Thomas et al., 1979; Cuffey & Paterson, 2010; Milillo et al., 2019). Over the past forty years of satellite observation, accelerated grounding-line retreat has largely occurred due to accelerated ice flux, resulting from thinning and collapse of ice shelves (Gudmandsson et al., 2019; Scheuchel et al., 2016) following an increase in ocean-forced melting (Pritchard et al., 2012). Much work has focused on describing ice-shelf thinning and resulting impacts (e.g. Rignot & Jacobs, 2002; Pattyn et al., 2006; Fürst et al., 2016; Adusumilli et al., 2020; Wei et al., 2020), finding that upstream ice-flux and grounding-line change is commonly non-linear and non-steady in space and time (Bamber & Dawson, 2020). Many other processes and conditions at grounding lines are largely unresolved (Powell & Alley, 1997; Schoof, 2007), such as their evolving shape and positionality (Horgan et al., 2013; Christianson et al., 2016; Simkins et al., 2018; Milillo et al., 2019).

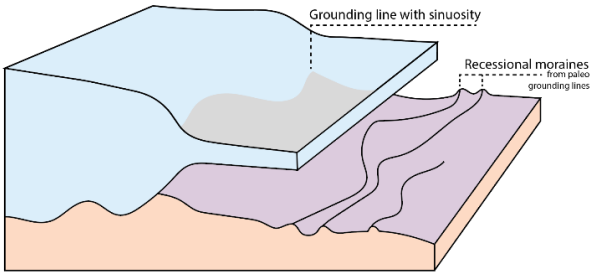

Grounding-line location is modulated by properties of the underlying bed and ice-flow behavior. Theory, models, and surveying of modern and paleo-grounding lines of the Antarctic Ice Sheet have shed light on basal conditions that impact grounding line behavior (Weertman, 1957; Anandakrishnan et al., 2007; Schoof et al., 2007; Katz & Worster, 2010; Bougamont et al., 2014; Jamieson et al., 2014; Christianson et al., 2016; Muto et al., 2019; Greenwood et al., 2021). Specifically, bed topography (Jakobsson et al., 2012; Favier et al., 2016; Sergienko & Wingham, 2019) - including the presence of pinning points (Fürst et al., 2015; Favier et al., 2016; Still & Hulbe, 2021) - slope (Jamieson et al., 2012; Joughin et al., 2014; refs), roughness (Siegert et al., 2004; Rippin et al., 2011), tidal-induced variability (Mohajerani et al., 2021), and geologic/lithologic composition (Parizek et al., 2013; Koellner et al., 2019) play a role in dictating grounding-line location. Additionally, the feedbacks between these properties and their influence on ice flow and meltwater production and transmission should be considered (Greenwood et al., 2021). However, all of these properties vary on spatial scales shorter than glacier catchment size. Similarly, ice-flow velocities are spatially and temporally variable with impacts on grounding line position (Hulbe & Fahnestock, 2004; Robel et al., 2014; Li et al., 2016). From first principles, catchment-scale ice-flow behaviour also impacts grounding-line location (Cuffey & Paterson, 2010). Changes in precipitation, lateral drag from sidewalls or shear margins, and buttressing from ice shelves and pinning points all force variations in ice thickness and discharge, which in turn set grounding-line location (Pattyn et al., 2006). Any force that produces spatial variations in longitudinal stretching or compression of ice near the grounding line will result in grounding-line sinuosity (Cuffey & Paterson, 2010). Ultimately, transitions in either bed properties or glacier catchment properties could drive small-scale variations in grounding line location and, in turn, advance or retreat of the grounding line can then lead to variations in ice flux across the grounding line as buttressing to inland grounded ice changes (Thomas et al., 1979).

Figure 1. Schematic of surficial and basal expressions of grounding lines and their change through time and space.

Heterogeneities in bed and glacier catchment properties could result in positional differences across the grounding line of individual glacial systems, so that

portions of an individual grounding line might be farther retreated or advanced than neighboring ice. From a plan-view perspective, this non-uniformity would manifest as longitudinal (i.e., lateral) sinuosity of grounding lines that conceptually increase ocean access to the grounding line, compared to a straight, linear grounding line (**Fig. 1**). We ask, do certain grounding-line configurations set up or reflect grounding line (in)stability and/or indicate heterogeneities in grounding-line conditions? Here, we explore the causes and significance of grounding-line sinuosity by coupling observations of contemporary Antarctic grounding lines and paleo-grounding lines expressed as ice-marginal landforms on the Ross Sea continental shelf (**Fig. 2a-b**), with an emphasis on the importance of subglacial bed properties (geology and topography) over glacier catchment properties (grounding line width and, for contemporary systems, ice flux, height above buoyancy, and buttressing). We then assess the relationship between sinuosity and multi-annual observations of grounding-line retreat where repeat satellite observations are available around the continent.

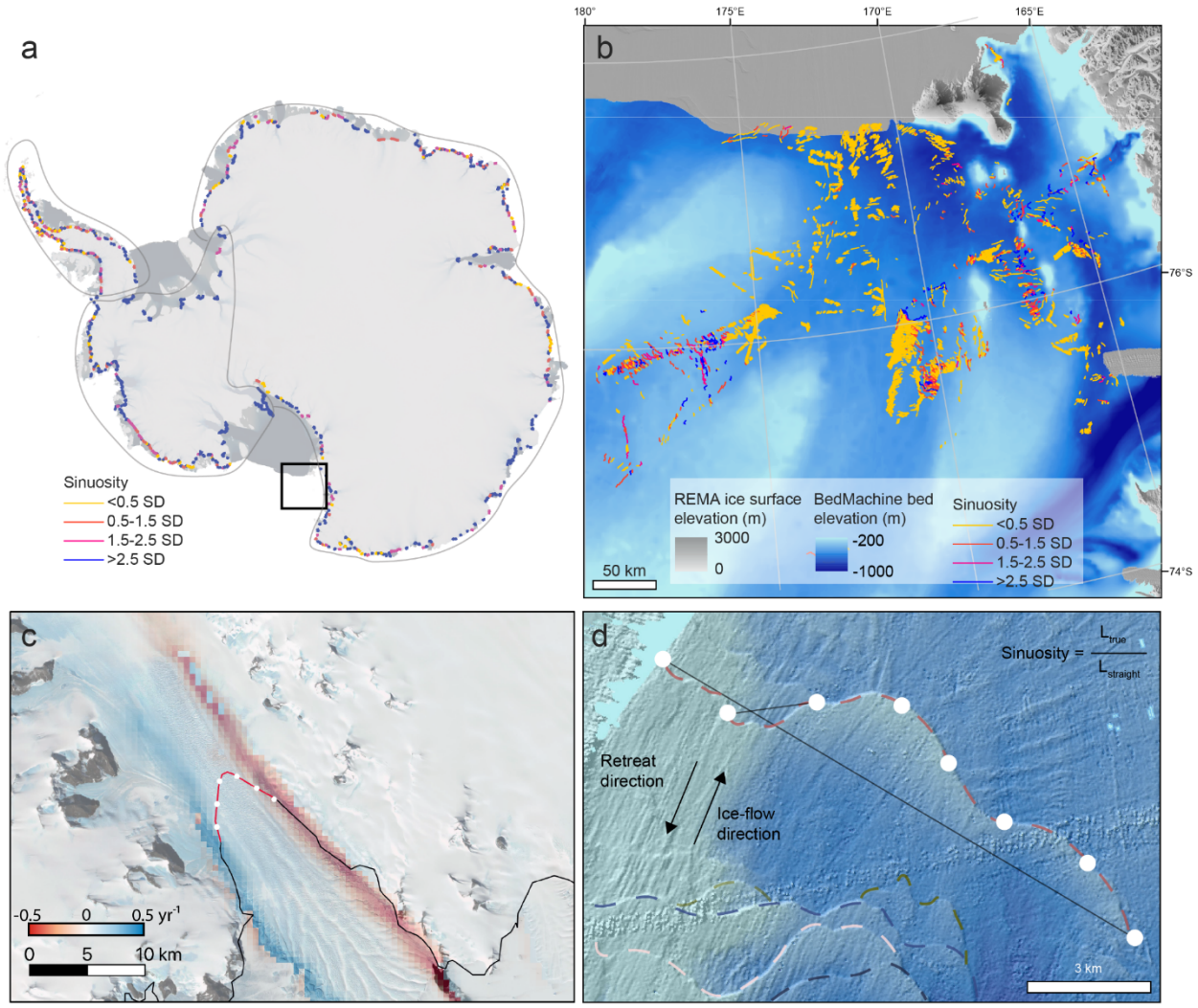

Fi

2. Spatial distribution of (a) modern grounding-line sinuosity (Rignot et al., 2016) and (b) paleo-grounding lines in the western Ross Sea (Simkins et al., 2018). Grounding lines in both (a) and (b) are colored by standard deviations (SD) of the full distribution of their respective datasets. The black box in (a) indicates the extent of (b). (c) An example of modern grounding-line sinuosity delineation for Pine Island Glacier. Sinuosity is calculated as the ratio of the true length, orthogonal to ice-flow direction, of the grounding lines and the straight line length between end-points. Individual system grounding lines (red line) are extracted from an ice-sheet wide product (Rignot et al., 2016; black line) between inflection points of the shear strain rate. (d) An example of paleo-grounding-line sinuosity in JOIDES Trough, western Ross Sea delineated by the true length of mapped ice-marginal landforms and the straight-line

length between landform end-points and for 2-km segments (white dots).

2 Data and Methods

We use modern grounding lines derived from the MEaSUREs Version 2 Differential Satellite Radar Interferometry dataset with spatial resolutions of 25-120 m spanning February 1992 to December 2014 (**Fig. 2a**; Rignot et al., 2016; Mouginot et al., 2017). The boundaries of individual grounding lines representative of individual glacier catchments (n=664) were delineated by the inflection points of the shear strain rate, $_{xy}$ (after Van der Veen et al., 2011; Dataset DOI: 10.15784/601484). Sinuosity was calculated as the ratio of the true length, orthogonal to ice-flow direction, of the grounding lines and the straight line length between end-points (**Fig. 2c**). Raster data were extracted at 1-km points along each grounding line and mean values were calculated for each grounding line.

A dataset of 6,275 paleo-grounding lines expressed as ice-marginal landforms on the deglaciated western Ross Sea continental shelf are used in this study, originally published by Simkins et al., 2018 (**Fig. 2b;** Dataset DOI: 10.15784/601484). The ice-marginal landforms were mapped from multibeam echo sounder data that was collected onboard the RVIB Nathaniel B. Palmer (NBP) 15-02 cruise using a Kongsberg EM122 operating in dual swath mode at 12 kHz frequency with 30-60% swath overlap (Cruise DOI: 10.7284/901477). The resulting bathymetry data was gridded at 20-40 m with decimeter vertical elevation resolution depending on water depth and sea-state. Sinuosity is calculated as a ratio of true (mapped) landform length, measured in the across paleo-ice flow direction at the crest of the landform, to the straight line distance between the mapped landform endpoints (**Fig. 2d**). Unlike the modern grounding lines that are fully mapped by satellites, the length of paleo-grounding lines is often incomplete (i.e., not the full grounding line length) due to the bounds of the surveyed area of the seafloor. Therefore, to compare modern and paleo-grounding lines, we opt to use a consistent length scale by segmenting the grounding lines into 2-km sections for the two datasets (modern, n=12,966; paleo, n=5,832; Dataset DOI: 10.15784/601484), even though this eliminates grounding lines that are less than 2-km long and thus results in 1 modern and 3,873 paleo-grounding lines removed (**Fig. 3**). For modern and paleo-grounding lines, sinuosity is consistently reported in units of km/km and thus we refer to sinuosity values in the text as unitless.

Average bed roughness for modern and paleo-grounding lines was calculated from BedMachine Antarctica (Morlighem et al., 2020) using the end- and mid-points of the 2-km segments and the native QGIS roughness algorithm, which calculates the largest inter-cell value between a central pixel and its surrounding pixels (BedMachine Antarctica has a pixel resolution of 500 m x 500 m). The BedMachine product is a modeled map of bed topography derived from mass conservation and constrained, where possible, from airborne radar observations of basal topography. As a result, roughness uncertainties range from 36 m to over 200 m (Morlighem, 2020) and the average uncertainty along the contemporary grounding lines we sampled is 49.2 m. Our results focus

more on bed topography gradients (slope, height-above-buoyancy gradient, bed roughness) rather than absolute elevation, for which there is more confidence in the mass-continuity approach. Average bed slope along ice-flow direction was similarly calculated using the end- and mid-points from BedMachine Antarctica and the MEaSUREs Version 2 Differential Satellite Radar Interferometry ice-flow directions (Rignot et al., 2017); however, for paleo-grounding lines, bed slope was averaged along the length of the grounding lines not in the direction of paleo-ice flow. For modern grounding lines, parameters were also averaged along the full grounding line length (**Fig. 4**), as well as being extracted at 2-km segments for a more direct comparison with the paleo grounding lines. Modern grounding lines were excluded in **Fig. 4** if their bed slope or roughness were more than two standard deviations greater than the mean

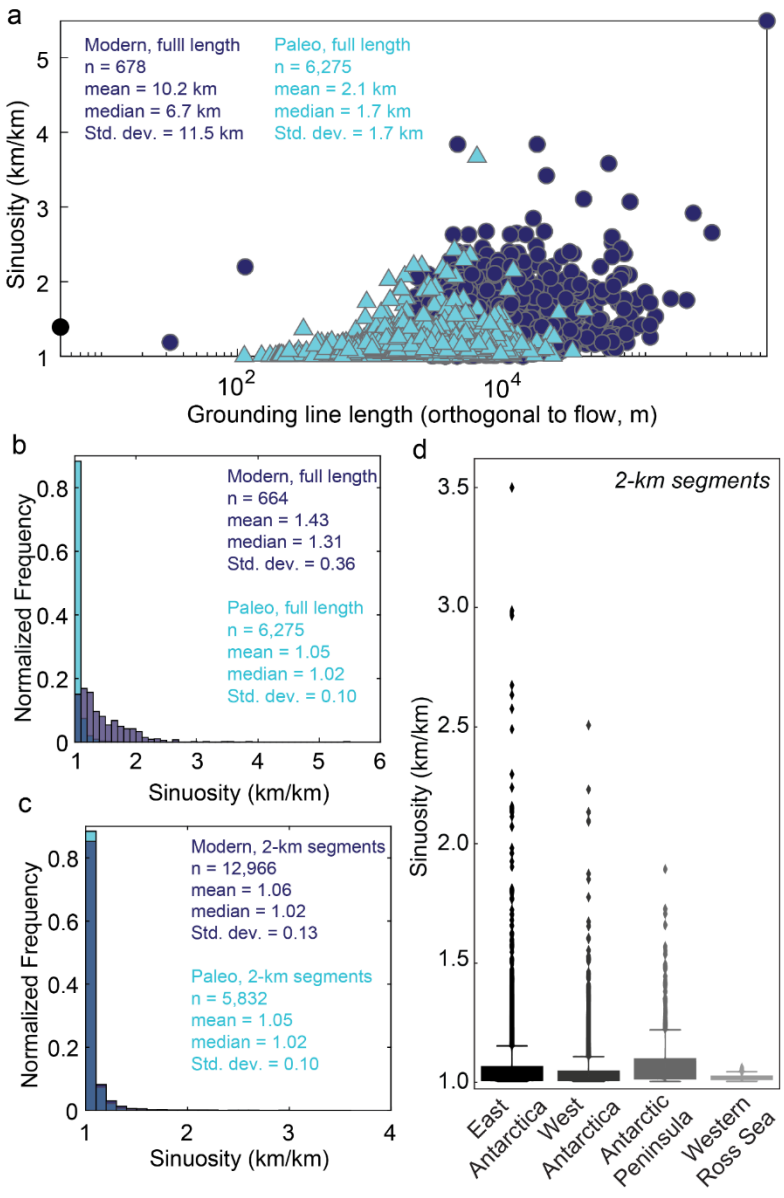

(17

degrees for bed slope and 433 m roughness).

Figure 3. (a) Sinuosity first increases and then becomes more scattered with increased grounding-line length. (b) Distribution of sinuosities for full-length grounding lines. (c) Because modern grounding lines are predominantly longer than mapped paleo-grounding lines, we compare the sinuosity of 2-km grounding line segments. (d) Box plots of grounding-line sinuosities for each region with the boxes representing the interquartile range, whiskers representing the minimum

and maximum 2-sigma values, and the points representing outliers. Grounding lines of regions defined as East Antarctica, West Antarctica and the Antarctic Peninsula are exclusively modern grounding lines, whereas grounding lines of the Western Ross Sea are exclusively paleo-grounding lines.

Additionally, for modern grounding lines, we assess glacier catchment properties including ice flux (Rignot et al., 2017) and ice-shelf presence/absence (Post et al., 2014), both available as datasets in Quantarctica Version 3 hosted by the Norwegian Polar Institute. Height-above buoyancy gradient was calculated (for each 2-km segment, as well as the full grounding line length) as a gradient parallel to ice-flow direction for a 5-km line, originating 5-km upstream of the grounding line and terminating at the grounding line; 1,345 anomalous, positive values were removed out of 12,966. We assume that glaciers approach flotation near their grounding line - otherwise stated, have a negative height above buoyancy gradient in the downstream direction - so any positive height-above-buoyancy gradients likely reflect uncertainty in the ice thickness data product and are removed. We additionally classified glaciers with prominent pinning points (i.e., bumps) at the grounding line based on the shape of the MEaSUREs grounding line by identifying, at some locations, clear topographic highs that cause large-scale undulations in the grounding line. Modern grounding-line retreat rates were calculated as area lost/gained between two time points with shear-margin defined glacier widths.

3 Results

Grounding-line sinuosity for modern and paleo-grounding lines appears to scale with grounding-line length, with fully resolved modern grounding lines ranging from $< 10^1$ m to nearly 10^5 m in length and mapped paleo-grounding lines ranging from 10^2 to $<10^5$ m in length (**Fig. 3a**). Despite the paleo-grounding lines being (presumably) only partially mapped, the ranges of length for modern and paleo-grounding lines are quite similar; however, the mean, median, and standard deviations are 4-, 5-, and 7-fold greater, respectively, for modern grounding lines. The sinuosity distributions for full-length grounding lines are drastically different, again with modern grounding lines being more sinuous and more variable than paleo-grounding lines (**Fig. 3b**). However, the segmented, 2-km long grounding lines have remarkably similar sinuosity distributions (**Fig. 3c**). This provides confidence in comparing and collectively assessing both modern and paleo-grounding lines and identifying sinuosity as a systematically characteristic property of grounding lines, independent of the grounding lines being contemporary or ancient. We hypothesize differences in sinuosity distributions in **Fig. 3b** arise from differences in their length as opposed to any fundamental differences between modern and paleo-grounding line processes.

Because regional tectonics and, more broadly, geologic history are a first-order control on bed topography and lithology, we might expect a geographic association with grounding-line sinuosity and regional bed properties. However, we find that there are not significant differences between the sinuosities of grounding lines grouped by tectonic-scale geology. We group grounding lines based

on geographic region (**Fig. 2a-b;** c.f., Rignot et al., 2019) including: West Antarctica (a Cretaceous to Cenozoic rift system with generally low elevation; Jordan et al., 2020); East Antarctica (a proterozoic craton with comparatively high elevation; Adie, 1962); the Antarctic Peninsula (a Mesozoic continental and magmatic arc system with Cenozoic accretion, thrusting, and volcanism; Ferraccioli et al., 2006); and the western Ross Sea (a series of extensional sedimentary basins, Cenozoic rifting and Quaternary volcanism; Davey, 1981; Copper et al., 1987). The East Antarctic grounding-line sinuosity population has larger outliers, while grounding lines of the Antarctic Peninsula span a slightly larger range in maximum values denoted by the extent of the upper whisker (**Fig. 3d**). However, the interquartile ranges of sinuosity distributions for East Antarctica, West Antarctica, and the Antarctic Peninsula have considerable overlap, rather than being disparate for distinct populations (**Fig. 3d**). This suggests that tectonic-scale geology is not a major predictor of or control on grounding-line sinuosity.

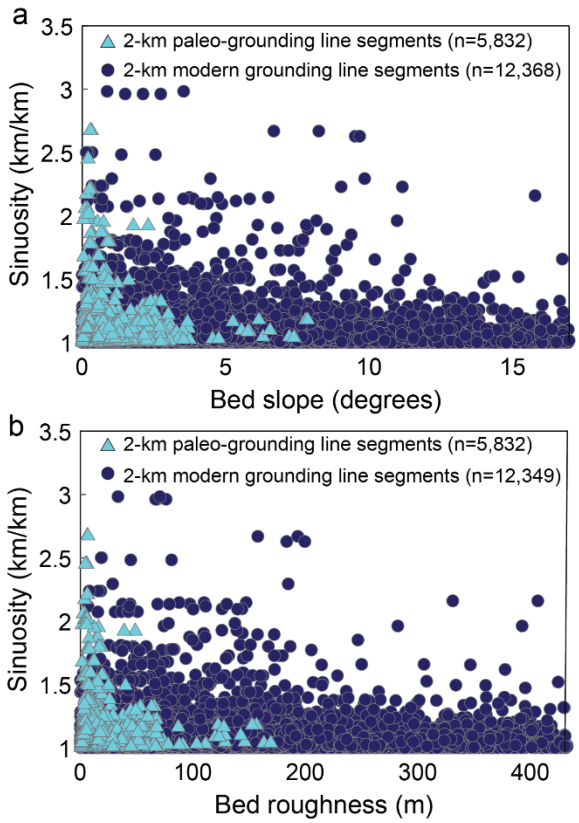

Figure 4. Distributions of (a) bed slope and (b) bed roughness for all 2-km grounding-line segments. (c) Bed slope association with sinuosity shows a preference of larger and more variable sinuosity on lower sloping beds and the greater spread of bed slopes on which modern grounding lines are situated. (d)

Similarly, lower bed roughness is associated with a larger range in sinuosity. For (c) and (d), modern grounding-line segments were excluded if their bed slope or roughness are greater than two standard deviations greater than the mean.

Across smaller spatial scales, we do see some degree of relationship between regional bed properties and grounding line sinuosity distributions. For example, paleo-grounding lines of the Ross Sea have fewer high-sinuosity outliers than grounding lines in other modern regions, which may reflect the influence of the sedimentary bed and relatively smooth topography of the western Ross Sea (**Fig. 2b**). Bed properties like slope and roughness - products of glacial histories and sediment erosion and deposition - impact and feedback on ice-flow velocity at and near grounding lines (e.g., Joughin & Alley, 2011) that may translate to grounding-line shape. Consistently for modern and paleo-grounding lines, higher and more variable sinuosity occurs on lower sloping beds (**Fig. 4a**). A remarkably similar relationship holds for bed roughness with lower bed roughness corresponding to higher and a larger range of grounding-line sinuosities (**Fig. 4b**). On lower sloping and roughness beds or, in other words, in the relative absence of (positive and negative) topographic relief, glacier catchment properties may be more important in dictating grounding line shape. Indeed, we find that greater sinuosity is associated with gradients in height-above-buoyancy that approach zero and are, thus, closer to floatation (**Fig. 5a**). Additionally, the majority of ice-flow velocities over 800 m a^{-1} occur at shallower height-above-buoyancy gradients, yet the fastest flowing glaciers seem to have a maximum sinuosity threshold of just over 2 (**Fig. 5a**). Other than a larger proportion of glaciers without ice shelves that have lower sinuosity, the mean and range (excluding outliers) of sinuosity for glaciers with and without ice shelves is very similar (**Fig. 5b**).

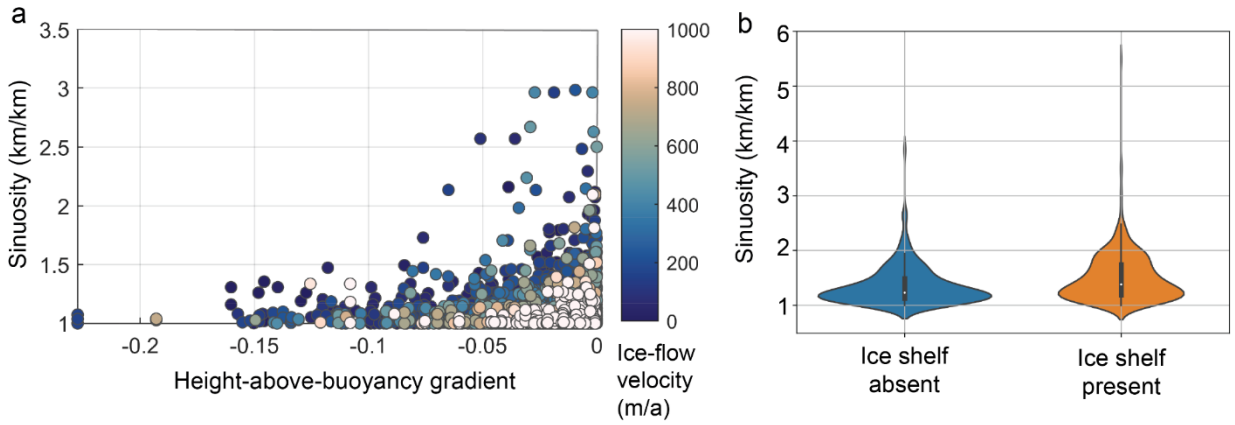

Fi

5. (a) Sinuosity of modern grounding lines, segmented at 2-km lengths, and ice-flow speeds increase as height-above-buoyancy gradient approaches 0. (b) Violin plot of sinuosity of full-length modern grounding lines for glaciers that terminate in an ice shelf and those that do not.

4 Discussion

While observational biases of paleo-grounding lines exist because many ice-marginal landforms are not fully surveyed, the sinuosity of the spatially limited subset of paleo-grounding lines described here is still representative of sinuosities observed across the full population of modern grounding lines (**Fig. 3c**). Around Antarctica, grounding lines most commonly approach linear with average sinuosity values for modern and paleo-grounding lines being 1.05 and 1.06, respectively (**Fig. 3c**). Regardless of geographic region, all grounding lines with sinuosity over 1.3 are identified as outliers; however, East Antarctic grounding lines have the largest spread in sinuosity outliers (**Fig. 3d**). We find that broadly defined geography (or rather tectonic history) is not a major control on grounding-line sinuosity, even though major regional differences, such as ice-sheet configuration and bed characteristics, exist. However, the paleo-grounding lines of the western Ross Sea have fewer high sinuosity outliers and a smaller interquartile range (**Fig. 3d**), which is the only region that is dominated by sediment basins and unlithified sediment cover (Halberstadt et al., 2018 and references therein) that may influence grounding-line behavior and morphology (Weertman, 1957; Alley et al., 1986).

We might expect that regions of high bed roughness would favor high grounding-line sinuosity as many small pinning points could force spatial variations in the position of grounding lines. However, conversely, we find that grounding lines on bed slopes less than ~2 degrees and on smoother beds with roughness less ~30 m have more pronounced and more variable sinuosity (**Fig. 4a-b**). Overall, the absence of pronounced topography seems to favor greater grounding-line sinuosity. However, sinuosity can also be similarly high for the 10% of grounding lines obviously pinned on positive topographic relief (**Fig. 6a**), as is the case for Pine Island Glacier before 2011 (Rignot et al., 2014) and the Whillans Ice Stream (**Fig. 6b**). This results in two settings that are associated with high sinuosity grounding lines: where beds are flat and smooth and where grounding lines are strongly pinned by topographic highs. Yet, the rarity of pinning points at contemporary grounding lines leaves the high sinuosity associated with pinning as outliers within the larger dataset and, interestingly, grounding lines situated on pinning points are not systematically on higher sloping or rougher beds (**Fig. 6c-d**).

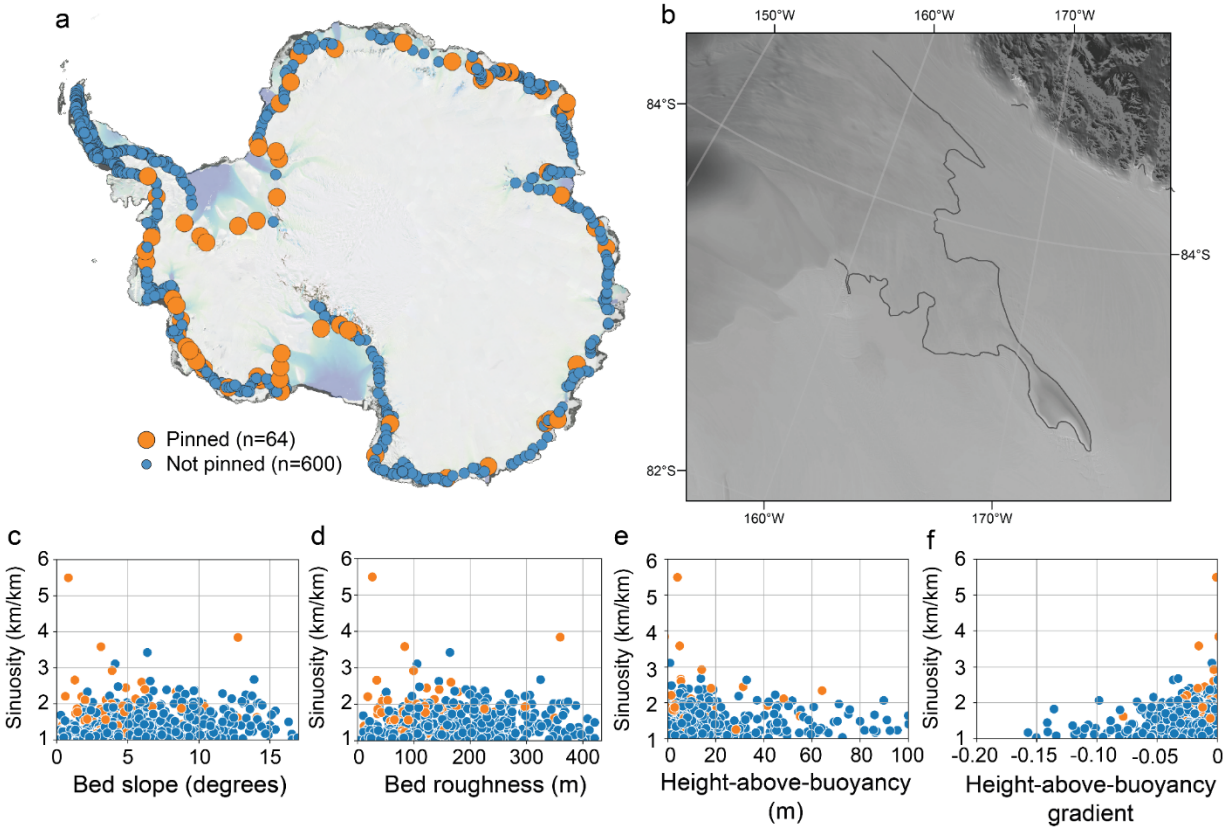

Figure 6. (a) Grounding lines clearly situated on pinning points (orange dots) around Antarctica are rare compared to grounding lines not clearly pinned (blue dots). (b) Example of a pinned grounding line is that of Whillans Ice Stream, with a grounding line that wraps around a pinning point at the downstream-most location of the grounding line. Scatter plots of full-length modern grounding line sinuosity, bed properties (c-d), and flotation (e-f) characteristics for modern grounding lines. All values are averages for the full grounding line.

The relationship between higher sinuosity with lower bed slope and roughness may reflect (or feedback on) glacier geometry, which is fundamental controls on grounding-line position (Cuffey & Paterson, 2010). The finding that lower height-above-buoyancy gradients are associated with greater sinuosity implies that contemporary grounding lines nearer to floatation are more susceptible to the development of sinuosity (**Fig. 5a**). Even for the rare grounding lines that are clearly pinned by positive topographic relief (**Fig. 6a**), higher, outlying sinuosities also correspond to lower height-above-buoyancy and lower height-above-buoyancy gradients (**Fig. 6e-f**). Additionally, the buttressing presence of an ice shelf does not seem to be particularly important in dictating sinuosity (**Fig. 5b**). We posit that lateral variability in grounding line po-

sition - expressed as sinuosity - largely results from the combined influence of ice thickness and bed slope which in turn set the height above buoyancy gradient and allow for small perturbations in the bed and glacier catchment to laterally shift grounding-line position. As a result, grounding-line sinuosity is more a product of minimal change in bed and glacier catchment properties. With grounding-line sinuosity impacted by bed and glacier geometry, what significance might sinuosity play in dictating or expressing glacier response to forcing?

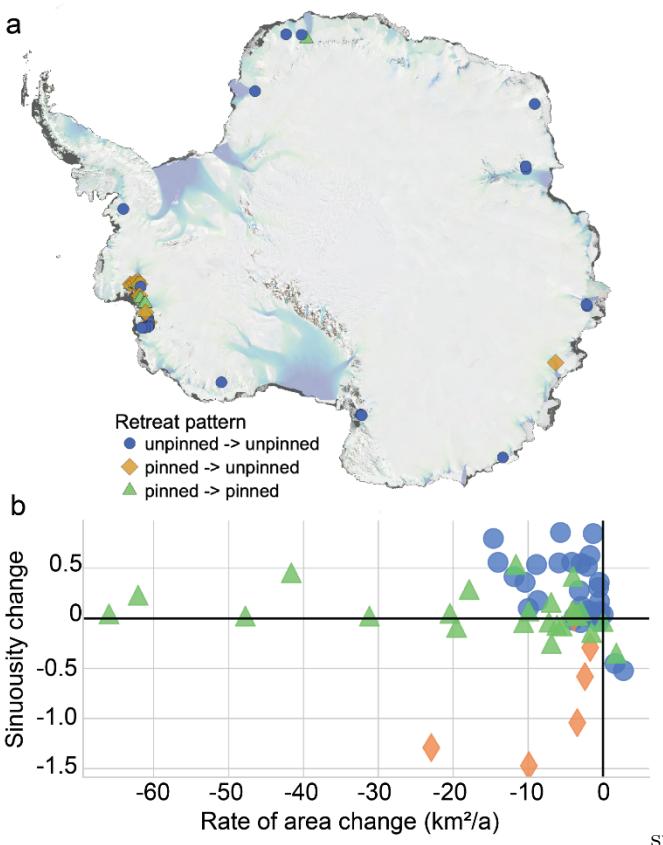

Figure 7. (a) The distribution of glaciers with two or more MEaSUREs grounding lines subdivided by whether grounding lines are unpinned, pinned, or transition from pinned to unpinned. (b) Relationship between rates of retreat (expressed as area change) and sinuosity change of grounding lines (Rignot et al., 2016), with negative rates indicating area loss.

For modern glaciers captured at two or more time points in the MEaSUREs dataset, we categorize by whether they are obviously pinned, unpinned, or transition from pinned to unpinned during retreat (**Fig. 7a**). Grounding lines that transition from pinned to unpinned during retreat experience a restricted range of rate of area loss (<25 km^2/a), while rates of area loss for

grounding lines that remain pinned throughout retreat exceed 60 km^2/a (**Fig. 7b**). In other words, unpinning of a grounding line from a prominent bed feature often results in a relatively small grounding-line retreat. Most of the pinned grounding lines are in the Amundsen Sea region and are undergoing rapid retreat due to ocean warming (e.g., Pritchard et al., 2012). We might expect that a grounding line pinned on a major topographic feature would be less sensitive to ocean-forced retreat and would have relatively low retreat rates. However, we find the opposite to be true in our small dataset: the presence of a pinning point at some location along a grounding line does not seem to reduce total grounding-line retreat, as pinned grounding lines retreat the most out of those studied here (**Fig. 7b**). Where retreat of grounding lines occurs gradually on the pinning point itself, rather than pulling off the pinning point, sinuosity changes minimally both in the positive and negative direction (green triangles in **Fig. 7b**). Greater loss of sinuosity scales with larger rates of area change for grounding lines that transition from pinned to unpinned (orange diamonds in **Fig. 7b**). The few advancing grounding lines (i.e., positive rates of area change) all lose sinuosity. For unpinned grounding lines around modern Antarctica, we find that sinuosity generally increases with grounding-line retreat (**Fig. 7b**). We, therefore, associate greater development of sinuosity with retreat of grounding lines not presumably stabilized by pinning points. However, sinuosity cannot perpetually increase. Insteads we suggest that most retreat events increase sinuosity for un-pinned grounding lines, with the occasional retreat event that broadly decreases and 'resets' sinuosity. This hypothesis is supported by broad-scale retreat patterns observed in the paleo-record (**Fig. 8**) and follows the work of Jamieson et al. (2012) who note the importance of lateral drag to "transient stabilizations" on reverse slopes. Furthermore, as low height-above-buoyancy gradients are less sensitive to marine ice-sheet instability and marine ice-cliff instability (Bassis et al., 2021), the majority of Antarctic grounding lines, which are unpinned on regionally smooth, flat beds may be more stable in positionality than pre-

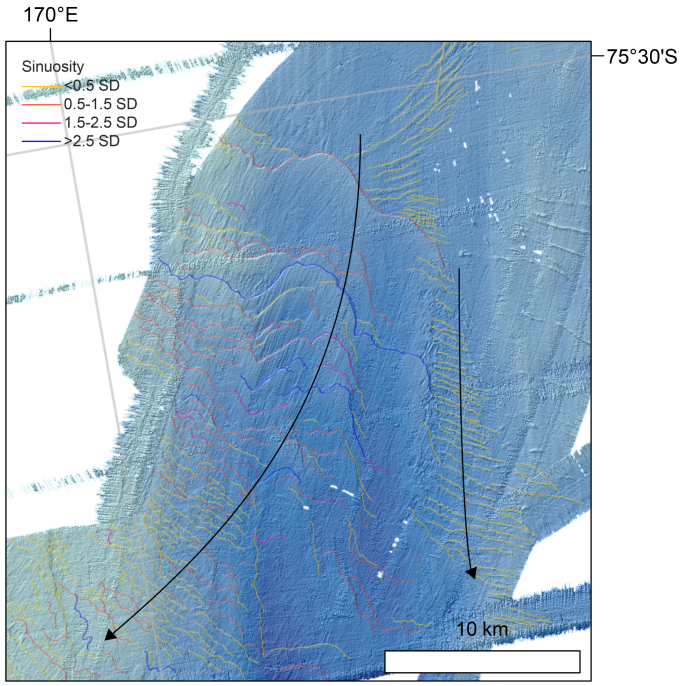

viously assumed (Gudmundsson et al., 2012; **Fig. 4**).

Figure 8. Paleo-grounding lines in JOIDES Trough in the western Ross Sea demonstrating sinuosity change in space and time during the retreat of a single paleo-ice stream. Black arrows denote directions of grounding-line retreat and thus older to younger time.

We find higher gains in sinuosity in unpinned configurations and greater losses in sinuosity when grounding lines lose their pinning points. Where grounding lines are strongly pinned (**Fig. 6a-b**), we hypothesize that greater sinuosity is a manifestation of differential lateral retreat, where the portion of the grounding line that is directly pinned is seaward of the rest of the grounding line that is farther retreated inland. Interestingly, those grounding lines that are pinned are near flotation (**Fig. 6e-f**) and could easily be forced to retreat by small amounts of thinning, as the entire grounding line is otherwise weakly grounded (Horgan & Anandakrishnan, 2006). This could then lead to a major change in the configuration of the grounding line and remove the heightened signature of bed-controlled sinuosity to result in a more linear (i.e., equally positioned) grounding line. Conversely, the development of greater sinuosity of unpinned grounding lines indicates that glacial or ocean conditions and/or processes are similarly capable of enhancing grounding line sinuosity. The most sinuous grounding lines are nearer to flotation (**Fig. 5a and 6e**) and thus potentially more susceptible to localized ocean-induced thinning and retreat (Christie et al., 2016). We suggest that sinuosity-induced embayments in unpinned grounding lines, similar to pinned grounding lines, reflect differential inland retreat. Therefore,

more linear grounding lines may indeed reflect fresher, newer grounding line positions (i.e., recent retreat to an inland location) as sinuosity has not developed yet due to spatiotemporal variability in processes and conditions at the grounding line. The paleo-record provides a substantially larger dataset than modern satellite-based records for observing variations in sinuosity through a retreat sequence. At a site recording retreat of a single unpinned ice stream on a relatively flat, smooth bed (**Fig. 8**), we see evidence for increasing grounding line sinuosity, constant sinuosity, and decreased sinuosity through time with retreat. In general, regions of large retreat magnitude between ice-marginal landforms have higher degrees of sinuosity variability than regions with more closely spaced landforms. In absence of dating from marine sediments, however, we do not have a timescale for the formation of these bedforms, so cannot make an equivalent comparison to modern grounding lines in terms of the relationship between retreat magnitude and sinuosity change. However, we can draw more general conclusions on the environmental factors contributing to sinuosity change across the retreat sequence. This suggests that variations in sinuosity at this site are primarily controlled by ice-flow dynamics and/or variable ocean properties, both of which can change abruptly in time and space at sub-glacier catchment scales.

5 Conclusions

The low sinuosity of the vast majority of Antarctic grounding lines, both in the modern and on the deglaciated continental shelf, reflects some consistency in the complex processes occurring at grounding lines. While most grounding lines approach linear in plan-view form, we find that enhanced sinuosity exists for low-sloping and low-roughness beds and where height-above-buoyancy gradients are shallow, regardless of pinning points and the presence or absence of an ice shelf. Sinuosity reflects differential inland retreat of individual grounding lines and perhaps sensitizes grounding lines for retreat via small amounts of thinning - either ocean-forced or through ice dynamics. Enhanced grounding-line sinuosity fundamentally increases grounding lines to ocean exposure, with more area of the grounding line in contact with seawater. Tidal effects on grounding line processes like subglacial melt are impacted by sinuosity of grounding lines, as the strength of ice limits tidal flexure within grounding line embayments (e.g. Wild et al., 2018); therefore, increased grounding-line sinuosity potentially amplifies tidal-influence processes, which may lead to retreat particularly on low-sloping beds. Depending on ice and bed slope, sinuosity-induced embayments may expose slightly thicker ice at the grounding line that could lead to locally increased ice flux across the grounding line, which for grounding lines near flotation could lead to enhanced retreat in those embayments. With the potential impacts of sinuosity on ocean exposure, tidal processes, and ice-flux at grounding lines, we demonstrate the need to understand lateral variability in grounding-line behavior and sub-catchment scale properties to assess the stability of grounding line positions today and in the future. Broadly, our study challenges the conceptual model of stable grounding line configurations only existing on prograde (i.e., normal, downstream-dipping) bed slopes or pinned subglacial topography.

Acknowledgements

Funded by a collaborative grant (NSF OPP 1745055) to L.M.S. and L.A.S., internal grants from University of Virginia to L.M.S., NSF OPP 1738934 to L.A.S. and NSF OPP 1739003 to K.L.R. We appreciate those who have contributed to open-source data and made this study possible. We thank [reviewers] and [editor] for constructive feedback. Data analysis and interpretation presented in this study was conducted in Charlottesville, Virginia on land that the Monacan Nation, in Lawrence, Kansas on the land of the Kaw, Kickapoo, Sioux, Ossage, and Shawnee, and in Corvallis, Oregon on the land of the Kalapuya, whom have protected and cultivated these lands for thousands of years, and the authors acknowledge their stewardship, past, present, and future.

Author contributions

L.M.S. conceptualized the study, curated data, carried out data analyses, contributed to data visualization, co-wrote the original draft, and acquired funding. L.A.S. curated data, carried out data analyses, contributed to data visualization, co-wrote the original draft, and acquired funding. K.L.R. carried out data analyses, contributed to data visualization, and co-wrote the original draft.

Open Research

Novel data presented here, inclusive of grounding line locations and metrics, are available as shapefiles and associated attribute tables and metrics used in the main text figures are provided in a spreadsheet, both of which are archived by the United States Antarctic Program Data Center, an online data repository for Antarctic projects funded by the National Science Foundation hosted by the Lamont-Doherty Earth Observatory of Columbia University (Dataset DOI: 10.15784/601484).

References

Adie, R. J. (1962, January). The geology of Antarctica. In *Antarctic research: the Matthew Fontaine Maury memorial symposium* (Vol. 7, pp. 26-39). Washington DC: American Geophysical Union.

Adusumilli, S., Fricker, H. A., Medley, B., Padman, L., & Siegfried, M. R. (2020). Interannual variations in meltwater input to the Southern Ocean from Antarctic ice shelves. *Nature geoscience*, *13*(9), 616-620.

Alley, R. B., Blankenship, D. D., Bentley, C. R., & Rooney, S. T. (1986). Deformation of till beneath ice stream B, West Antarctica. *Nature*, *322*(6074), 57-59.

Anandakrishnan, S., Catania, G. A., Alley, R. B., & Horgan, H. J. (2007). Discovery of till deposition at the grounding line of Whillans Ice Stream. *Science*, *315*(5820), 1835-1838.

Bamber, J. L., & Dawson, G. J. (2020). Complex evolving patterns of mass loss from Antarctica's largest glacier. *Nature Geoscience*, *13*(2), 127-131.

Bassis, J. N., Berg, B., Crawford, A. J., & Benn, D. I. (2021). Transition to marine ice cliff instability controlled by ice thickness gradients and velocity. *Science*, *372*(6548), 1342-1344.

Bougamont, M., Christoffersen, P., Hubbard, A. L., Fitzpatrick, A. A., Doyle, S. H., & Carter, S. P. (2014). Sensitive response of the Greenland Ice Sheet to surface melt drainage over a soft bed. *Nature communications*, *5*(1), 1-9.

Christianson, K., Jacobel, R. W., Horgan, H. J., Alley, R. B., Anandakrishnan, S., Holland, D. M., & DallaSanta, K. J. (2016). Basal conditions at the grounding zone of Whillans Ice Stream, West Antarctica, from ice-penetrating radar. *Journal of Geophysical Research: Earth Surface*, *121*(11), 1954-1983.

Christie, F. D., Bingham, R. G., Gourmelen, N., Tett, S. F., & Muto, A. (2016). Four-decade record of pervasive grounding line retreat along the Bellingshausen margin of West Antarctica. *Geophysical Research Letters*, 43(11), 5741-5749.

Cooper, A. K., Barrett, P. J., Hinz, K., Traube, V., Letichenkov, G., & Stagg, H. M. (1991). Cenozoic prograding sequences of the Antarctic continental margin: a record of glacio-eustatic and tectonic events. *Marine Geology*, *102*(1-4), 175-213.

Cuffey, K. M., & Paterson, W. S. B. (2010). The physics of glaciers. Academic Press.

Davey, F. J. (1981). Geophysical studies in the Ross Sea region. *Journal of the Royal Society of New Zealand*, *11*(4), 465-479.

Favier, L., Pattyn, F., Berger, S., & Drews, R. (2016). Dynamic influence of pinning points on marine ice-sheet stability: a numerical study in Dronning Maud Land, East Antarctica. *The Cryosphere*, *10*(6), 2623-2635.

Ferraccioli, F., Jones, P. C., Vaughan, A. P. M., & Leat, P. T. (2006). New aerogeophysical view of the Antarctic Peninsula: More pieces, less puzzle. *Geophysical Research Letters*, *33*(5).

Fürst, J. J., Durand, G., Gillet-Chaulet, F., Merino, N., Tavard, L., Mouginot, J., ... & Gagliardini, O. (2015). Assimilation of Antarctic velocity observations provides evidence for uncharted pinning points. *The Cryosphere*, *9*(4), 1427-1443.

Fürst, J. J., Durand, G., Gillet-Chaulet, F., Tavard, L., Rankl, M., Braun, M., & Gagliardini, O. (2016). The safety band of Antarctic ice shelves. *Nature Climate Change*, *6*(5), 479-482.

Greenwood, S. L., Simkins, L. M., Winsborrow, M. C., & Bjarnadóttir, L. R. (2021). Exceptions to bed-controlled ice sheet flow and retreat from glaciated continental margins worldwide. *Science advances*, *7*(3), eabb6291.

Gudmundsson, G. H., Krug, J., Durand, G., Favier, L., & Gagliardini, O. (2012). The stability of grounding lines on retrograde slopes. *The Cryosphere*, *6*(6), 1497-1505.

Halberstadt, A. R. W., Simkins, L. M., Anderson, J. B., Prothro, L. O., & Bart, P. J. (2018). Characteristics of the deforming bed: till properties on the deglaciated Antarctic continental shelf. *Journal of Glaciology*, *64*(248), 1014-1027.

Horgan, H. J., & Anandakrishnan, S. (2006). Static grounding lines and dynamic ice streams: Evidence from the Siple Coast, West Antarctica. *Geophysical Research Letters*, *33*(18).

Horgan, H. J., Christianson, K., Jacobel, R. W., Anandakrishnan, S., & Alley, R. B. (2013). Sediment deposition at the modern grounding zone of Whillans Ice Stream, West Antarctica. *Geophysical Research Letters*, *40*(15), 3934-3939.

Hulbe, C. L., & Fahnestock, M. A. (2004). West Antarctic ice-stream discharge variability: mechanism, controls and pattern of grounding-line retreat. *Journal of Glaciology*, *50*(171), 471-484.

Jakobsson, M., Anderson, J. B., Nitsche, F. O., Gyllencreutz, R., Kirshner, A. E., Kirchner, N., ... & Eriksson, B. (2012). Ice sheet retreat dynamics inferred from glacial morphology of the central Pine Island Bay Trough, West Antarctica. *Quaternary Science Reviews*, *38*, 1-10.

Jamieson, S. S., Vieli, A., Livingstone, S. J., Cofaigh, C. Ó., Stokes, C., Hillenbrand, C. D., & Dowdeswell, J. A. (2012). Ice-stream stability on a reverse bed slope. *Nature Geoscience*, *5*(11), 799-802.

Jamieson, S. S., Vieli, A., Cofaigh, C. Ó., Stokes, C. R., Livingstone, S. J., & Hillenbrand, C. D. (2014). Understanding controls on rapid ice-stream retreat during the last deglaciation of Marguerite Bay, Antarctica, using a numerical model. *Journal of Geophysical Research: Earth Surface*, *119*(2), 247-263.

Jordan, T. A., Riley, T. R., & Siddoway, C. S. (2020). The geological history and evolution of West Antarctica. *Nature Reviews Earth & Environment*, *1*(2), 117-133.

Joughin, I., Smith, B. E., & Medley, B. (2014). Marine ice sheet collapse potentially under way for the Thwaites Glacier Basin, West Antarctica. *Science*, *344*(6185), 735-738.

Joughin, I., & Alley, R. B. (2011). Stability of the West Antarctic ice sheet in a warming world. *Nature Geoscience*, *4*(8), 506-513.

Katz, R. F., & Worster, M. G. (2010). Stability of ice-sheet grounding lines. *Proceedings of the Royal Society A: Mathematical, Physical and Engineering Sciences*, *466*(2118), 1597-1620.

Koellner, S., Parizek, B. R., Alley, R. B., Muto, A., & Holschuh, N. (2019). The impact of spatially-variable basal properties on outlet glacier flow. *Earth and Planetary Science Letters*, *515*, 200-208.

Li, X., Rignot, E., Mouginot, J., & Scheuchl, B. (2016). Ice flow dynamics and mass loss of Totten Glacier, East Antarctica, from 1989 to 2015. *Geophysical*

Research Letters, *43*(12), 6366-6373.

Milillo, P., Rignot, E., Rizzoli, P., Scheuchl, B., Mouginot, J., Bueso-Bello, J., & Prats-Iraola, P. (2019). Heterogeneous retreat and ice melt of Thwaites Glacier, West Antarctica. *Science advances*, *5*(1), eaau3433.

Mohajerani, Y., Jeong, S., Scheuchl, B., Velicogna, I., Rignot, E., & Milillo, P. (2021). Automatic delineation of glacier grounding lines in differential interferometric synthetic-aperture radar data using deep learning. *Scientific reports*, *11*(1), 1-10.

Muto, A., Anandakrishnan, S., Alley, R. B., Horgan, H. J., Parizek, B. R., Koellner, S., ... & Holschuh, N. (2019). Relating bed character and subglacial morphology using seismic data from Thwaites Glacier, West Antarctica. *Earth and Planetary Science Letters*, *507*, 199-206.

Mouginot, J., B. Scheuchl, and E. Rignot. 2017. MEaSUREs Antarctic Boundaries for IPY 2007-2009 from Satellite Radar, Version 2. [Indicate subset used]. Boulder, Colorado USA. NASA National Snow and Ice Data Center Distributed Active Archive Center. http://dx.doi.org/10.5067/AXE4121732AD.

Parizek, B. R., Christianson, K., Anandakrishnan, S., Alley, R. B., Walker, R. T., Edwards, R. A., ... & Nowicki, S. M. J. (2013). Dynamic (in) stability of Thwaites Glacier, West Antarctica. *Journal of Geophysical Research: Earth Surface*, *118*(2), 638-655.

Pattyn, F., Huyghe, A., De Brabander, S., & De Smedt, B. (2006). Role of transition zones in marine ice sheet dynamics. *Journal of Geophysical Research: Earth Surface*, *111*(F2).

Post, A.L., Meijers, A.J.S., Fraser, A.D., Meiners, K.M., Ayers, J., Bindoff, N.L., … & Raymond, B., 2014. Chapter 14. Environmental Setting, In: De Broyer, C., Koubbi, P., Griffiths, H.J., Raymond, B., d'Udekem d'Acoz, C., et al. (Eds.), Biogeographic Atlas of the Southern Ocean. Scientific Committee on Antarctic Research, Cambridge, pp. 46-64.

Powell RD, Alley RB. 1997. Grounding-line systems: processes, glaciological inferences and the stratigraphic record. In Geology and Seismic Stratigraphy of the Antarctic Margin, Barker PF, Cooper AK (eds). Antarctic Research Series 2: 169–187. Geological Society, London.

Pritchard, H., Ligtenberg, S. R., Fricker, H. A., Vaughan, D. G., van den Broeke, M. R., & Padman, L. (2012). Antarctic ice-sheet loss driven by basal melting of ice shelves. *Nature*, *484*(7395), 502-505.

Rignot, E., & Jacobs, S. S. (2002). Rapid bottom melting widespread near Antarctic ice sheet grounding lines. *Science*, *296*(5575), 2020-2023.

Rignot, E., Mouginot, J., Morlighem, M., Seroussi, H., & Scheuchl, B. (2014). Widespread, rapid grounding line retreat of Pine Island, Thwaites, Smith, and

Kohler glaciers, West Antarctica, from 1992 to 2011. *Geophysical Research Letters*, *41*(10), 3502-3509.

Rignot, E., Mouginot, J. & Scheuchl, B. (2016). MEaSUREs Antarctic Grounding Line from Differential Satellite Radar Interferometry, Version 2. Boulder, Colorado USA. NASA National Snow and Ice Data Center Distributed Active Archive Center. doi: https://doi.org/10.5067/IKBWW4RYHF1Q.

Rignot, E., Mouginot, J. & Scheuchl, B. (2017). MEaSUREs InSAR-Based Antarctica Ice Velocity Map, Version 2. Boulder, Colorado USA. NASA National Snow and Ice Data Center Distributed Active Archive Center. doi: https://doi.org/10.5067/D7GK8F5J8M8R.

Rignot, E., Mouginot, J., Scheuchl, B., Van Den Broeke, M., Van Wessem, M. J., & Morlighem, M. (2019). Four decades of Antarctic Ice Sheet mass balance from 1979–2017. *Proceedings of the National Academy of Sciences*, *116*(4), 1095-1103.

Rippin, D. M., Vaughan, D. G., & Corr, H. F. (2011). The basal roughness of Pine Island Glacier, West Antarctica. *Journal of Glaciology*, *57*(201), 67-76.

Robel, A. A., Schoof, C., & Tziperman, E. (2014). Rapid grounding line migration induced by internal ice stream variability. *Journal of Geophysical Research: Earth Surface*, *119*(11), 2430-2447.

Scheuchl, B., Mouginot, J., Rignot, E., Morlighem, M., & Khazendar, A. (2016). Grounding line retreat of Pope, Smith, and Kohler Glaciers, West Antarctica, measured with Sentinel-1a radar interferometry data. *Geophysical Research Letters*, *43*(16), 8572-8579.

Schoof, C. (2007). Ice sheet grounding line dynamics: Steady states, stability, and hysteresis. *Journal of Geophysical Research: Earth Surface*, *112*(F3).

Sergienko, O. V., & Wingham, D. J. (2019). Grounding line stability in a regime of low driving and basal stresses. *Journal of Glaciology*, *65*(253), 833-849.

Siegert, M. J., Taylor, J., Payne, A. J., & Hubbard, B. (2004). Macro-scale bed roughness of the siple coast ice streams in West Antarctica. *Earth Surface Processes and Landforms: The Journal of the British Geomorphological Research Group*, *29*(13), 1591-1596.

Simkins, L. M., Greenwood, S. L., & Anderson, J. B. (2018). Diagnosing ice sheet grounding line stability from landform morphology. *The Cryosphere*, *12*(8), 2707-2726.

Still, H., & Hulbe, C. (2021). Mechanics and dynamics of pinning points on the Shirase Coast, West Antarctica. *The Cryosphere*, *15*(6), 2647-2665.

Thomas, R. (1979). The Dynamics of Marine Ice Sheets. *Journal of Glaciology, 24*(90), 167-177. doi:10.3189/S0022143000014726

Van der Veen, C. J., J. C. Plummer, & L. A. Stearns. (2011). Controls on the recent speed up of Jakobshavn Isbræ, West Greenland. *Journal of Glaciology*, 57(204), 770-782

Weertman, J. (1957). On the sliding of glaciers. *Journal of Glaciology*, *3*(21), 33-38.

Wei, W., Blankenship, D. D., Greenbaum, J. S., Gourmelen, N., Dow, C. F., Richter, T. G., ... & Assmann, K. M. (2020). Getz Ice Shelf melt enhanced by freshwater discharge from beneath the West Antarctic Ice Sheet. *The Cryosphere*, *14*(4), 1399-1408.

Wild, C. T., Marsh, O. J., & Rack, W. (2018). Unraveling InSAR observed Antarctic ice-shelf flexure using 2-D elastic and viscoelastic modeling. *Frontiers in Earth Science*, *6*, 28.